NANO LETTERS

Letter

pubs.acs.org/NanoLett

Engineering Nanoparticle-Coated Bacteria as Oral DNA Vaccines for Cancer Immunotherapy

Qinglian Hu,[†,⊥] Min Wu,[†,⊥] Chun Fang,[‡] Changyong Cheng,[‡] Mengmeng Zhao,[†] Weihuan Fang,[‡] Paul K. Chu,[§] Yuan Ping,*[,∥] and Guping Tang*[,†]

[†]Institute of Chemical Biology and Pharmaceutical Chemistry, Zhejiang University, Hangzhou 310028, China

[‡]College of Animal Science, Zhejiang University, Hangzhou 310028, China

[§]Department of Physics and Materials Science, City University of Hong Kong, Tat Chee Avenue, Kowloon, Hong Kong, China

[∥]School of Materials Science and Engineering, Nanyang Technological University, Singapore 639798, Singapore

Supporting Information

ABSTRACT: Live attenuated bacteria are of increasing importance in biotechnology and medicine in the emerging field of cancer immunotherapy. Oral DNA vaccination mediated by live attenuated bacteria often suffers from low infection efficiency due to various biological barriers during the infection process. To this end, we herein report, for the first time, a new strategy to engineer cationic nanoparticle-coated bacterial vectors that can efficiently deliver oral DNA vaccine for efficacious cancer immunotherapy. By coating live attenuated bacteria with synthetic nanoparticles self-assembled from cationic polymers and plasmid DNA, the protective nanoparticle coating layer is able to facilitate bacteria to effectively escape phagosomes, significantly enhance the acid tolerance of bacteria in stomach and intestines, and greatly promote dissemination of bacteria into blood circulation after oral administration. Most importantly, oral delivery of DNA vaccines encoding autologous vascular endothelial growth factor receptor 2 (VEGFR2) by this hybrid vector showed remarkable T cell activation and cytokine production. Successful inhibition of tumor growth was also achieved by efficient oral delivery of VEGFR2 with nanoparticle-coated bacterial vectors due to angiogenesis suppression in the tumor vasculature and tumor necrosis. This proof-of-concept work demonstrates that coating live bacterial cells with synthetic nanoparticles represents a promising strategy to engineer efficient and versatile DNA vaccines for the era of immunotherapy.

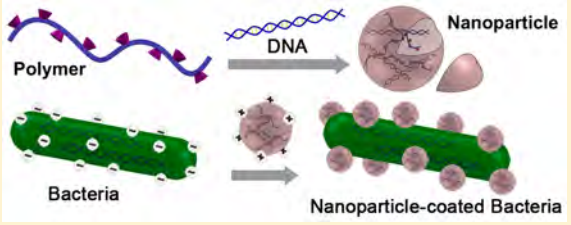

KEYWORDS: *hybrid living material, Salmonella, phagosomal escape, acid tolerance, cationic polymer, vaccine delivery*

Immunotherapy has received considerable attention as an emerging cancer therapy modality, as this therapeutic strategy is of great potential in terms of its ability to break the immune tolerance and evoke an immune response to target cancer cells with much less side effects.[1−3] Although oral delivery of DNA vaccine represents one of the most promising approaches in cancer immunotherapy;[4,5] however, the low levels of DNA transfection is the main problem limiting efficacious immune response.[6−8] Live attenuated strains of a few bacteria have been developed as vaccines for a number of infectious diseases and several types of cancers and were also exploited as potential vaccine vectors to delivery different types of antigenic messages for activating antitumor immune responses.[9−11] For example, *Salmonellae* harboring cancer-specific antigen-expressing plasmid has been shown to be effective in DNA delivery and efficacious in the subsequent induction of immunity against antigens encoded by the plasmid.[5,12,13] Attenuated *Salmonella* vaccines have been successfully used as carriers for the oral delivery of vaccines.[4,14] As compared to bacterial vaccines delivered via intravenous injection, oral vaccination mediated by *attenuated Salmonella* is cost-effective and less toxic.[15−17] Orally administered *Salmonellae* are able to colonize the gut-associated lymphoid tissue through the microfold cells of Peyer's patches initially, where they could be engulfed and processed by dendritic cells or macrophages to stimulate a strong and durable immunological response.[18] Subsequently, the rest bacteria drain through the lymphatics to the thoracic duct into the blood and ultimately infect the liver and spleen, where they replicate inside phagocytic cells and also induce an innate immune response.[19] However, the oral infection efficiency of *Salmonellae* is often low, due to the digestion of live attenuated *Salmonellae* in the acidic stomach environment.[20] Additionally, *Salmonellae* lack the ability to escape phagosomes after they are captured by phagocytes, which has severely restricted its replication within macrophages following the invasion into intestinal mucosa.[18] As a result, the induction of MHC class-I-restricted immune response is largely limited, which is the key reason for the failure of DNA vaccination against cancer.[21,22] Collectively, it is of paramount importance to develop highly effective vectors to overcome current hurdles of oral DNA vaccine delivery.

Received: February 10, 2015
Revised: March 20, 2015
Published: March 25, 2015

DOI: 10.1021/acs.nanolett.5b00570
Nano Lett. 2015, 15, 2732−2739

Scheme 1. Schematic Illustration of the Cationic Nanoparticle-Coated Attenuated *Salmonellae* for Improved Antigen Expression and Tumor Targeting Immune Responsive Activation[a]

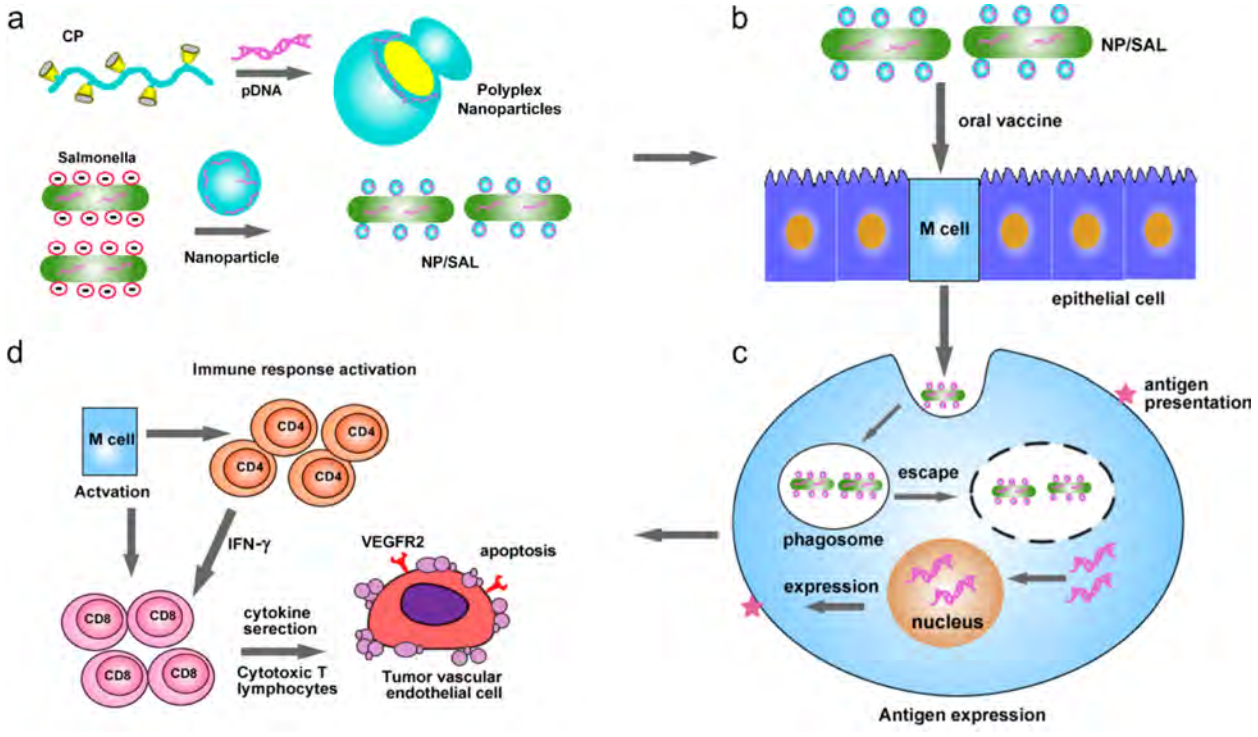

[a](a) Engineering of polyplex nanoparticle-coated *Salmonellae*. (b) Oral DNA vaccine delivery mediated by nanoparticle-coated *Salmonellae*. (c) Intracellular trafficking of nanoparticle-coated *Salmonellae* and antigen expression. (d) Activation of antitumor immune response.

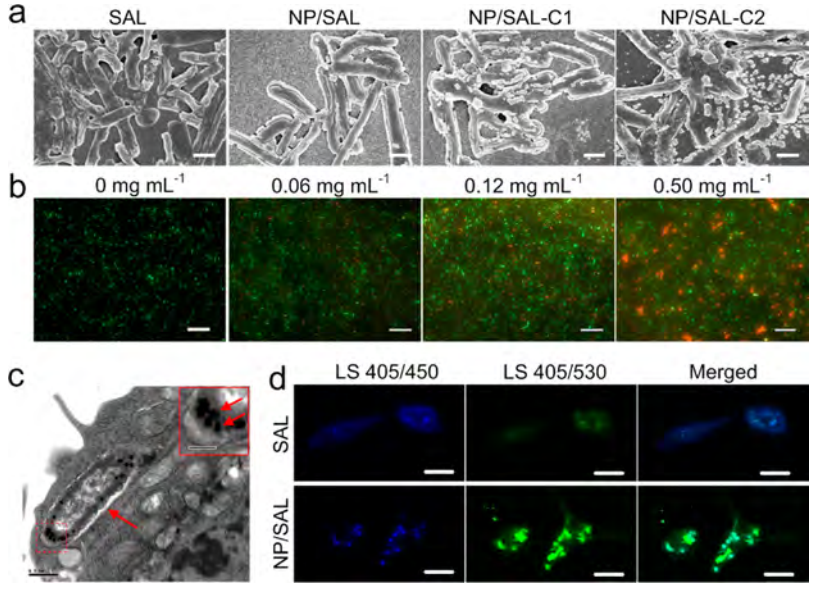

Figure 1. (a) Morphology of naked *Salmonellae* and coated *Salmonellae* with different concentrations of polyplex nanoparticles, as observed by scanning electron microscopy. The scale bars represent 1 μm. (b) Fluorescence microscopic images of the attenuated *Salmonella* incubated with different concentrations of polyplex nanoparticles. The *Salmonella* (2×10^6 CFU/mL) was coated with 0 mg/mL, 0.06 mg/mL (NP/SAL), 0.12 mg/mL (NP/SAL-C1), and 0.50 mg/mL (NP/SAL-C2) of polyplex nanoparticles. Naked bacteria with green fluorescence represent the intact cell membrane, whereas those in red represent damaged cell membrane. The live and dead *Salmonellae* were stained by LIVE/DEAD BacLight bacterial viability kits. The scale bars represent 50 μm. (c) TEM image of the intracellular location of NP/SAL in the RAW 264.7 cells. The scale bar represents 0.5 μm (image) and 0.2 μm (insert), respectively. The arrows denote the internalized coated bacteria (image) and nanoparticles adherent to bacteria (insert), respectively. (d) Infection of peritoneal macrophage mediated by NP/SAL and *Salmonellae*. The cells were stained by LysoSensor Yellow/Blue DND-160 after infection. The scale bars represent 20 μm.

"Living materials" that combine the advantages of living cells with nonliving nanomaterials are emerged as a new class of functional materials in the past few years. The intrinsic features of live bacterial cells with the merits of synthetic materials provides

DOI: 10.1021/acs.nanolett.5b00570
Nano Lett. 2015, 15, 2732−2739

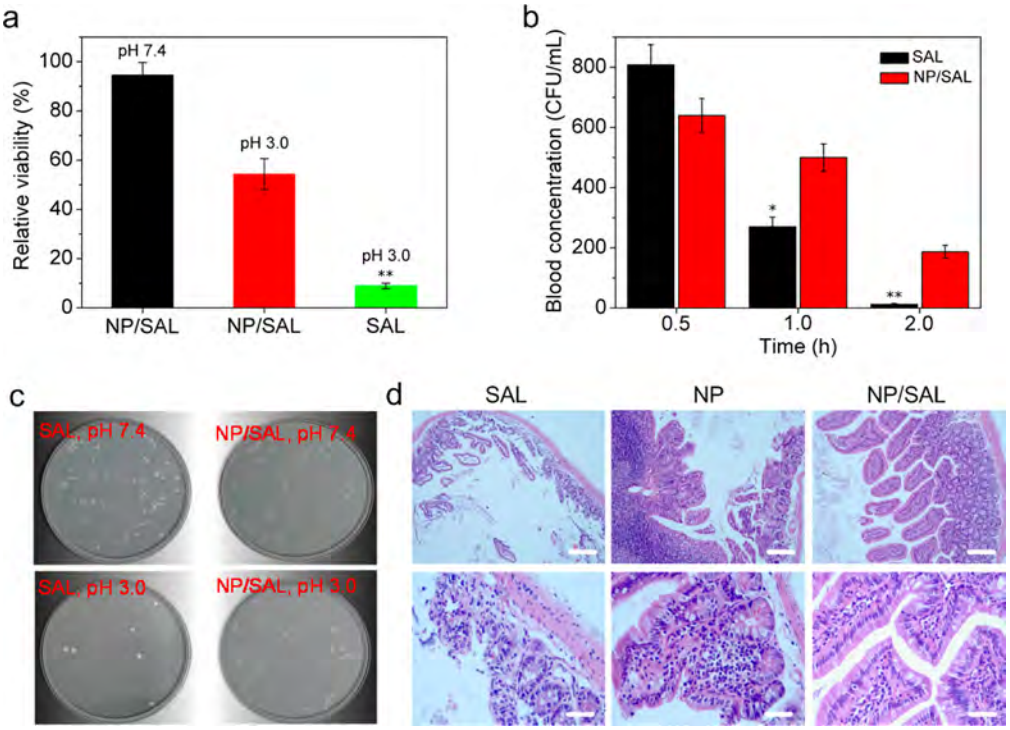

Figure 2. (a) Relative viability of NP/SAL and uncoated *Salmonellae* at physiological pH (pH 7.4) and simulated stomach pH (pH 3.0). The absolute number of viable *Salmonellae* was defined as 100%. Data represent mean ± SD ($n = 3$, Student's t test, $^{**}P < 0.01$, SAL (pH3.0) vs NP/SAL (pH3.0)). (b) Blood concentration of *Salmonellae* and NP/SAL at different time points after oral administration. Data represent mean ± SD, and comparison of group means was made between SAL group and NP/SAL group at the same time point after oral administration. ($n = 3$, Student's t test, $^{*}P < 0.05$, $^{**}P < 0.01$) (c) Growth of uncoated and coated *Salmonellae* in Petri plates after exposure to different pH buffers. (d) H&E stained small intestine section of mice treated with *Salmonella*, NP or NP/SAL by oral administration successively for 3 days. The scale bar represents 200 μm (upper panel ×100; lower panel ×400).

the potential for several applications such as electricity conducting and light emitting, cell imaging and barcoding, as well as pathogen detection.[23−25] Synthetic polymer-coated live bacteria were also designed for damaging cancer cells with multimodal features and modulating tumor-targeting efficiency.[26,27] Furthermore, bacteria-mediated nanoparticle and cargo delivery approach (termed as microbotics) also exhibited excellent potential for the delivery of nucleic acids by taking advantages of the invasive nature of bacteria.[28] Inspired by these works, we attempt to coat *Salmonella* with nanoparticles self-assembled from cationic polymers and DNA in overcoming multiple barriers in the oral delivery of DNA vaccines. Cationic polymers represent a promising type of nonviral gene delivery vectors and are able to spontaneously complex with DNA (or other nucleic acids) to form nanoscaled polymer/DNA complexes (polyplexes) through electrostatic interactions.[29] The strong buffering capacity of cationic polymers could effectively help themselves escape from endo/lysosome as a result of "proton sponge" effect.[30,31] For example, 25 kDa polyethylenimine (PEI) is well known for its excellent transfection activity in vitro largely due to its strong buffering capacity. The PEI/DNA complexes escape the endosomal through a "proton-sponge" mechanism.[32] Similarly, cross-linked β-cyclodextrin-PEI600 (CP) with degradable PEI network was demonstrated as an efficient vector for nucleic acid delivery in vitro and in vivo in our previous study.[33−36] On the basis of the merits of cationic polymers, we herein disclose that a living hybrid system composed of synthetic CP nanoparticles and live attenuated *Salmonellae* acts as an efficient vector to deliver oral DNA vaccines and achieves potent antitumor immune response in vivo. The nanoparticle-coated *Salmonella* we developed is expect to fullfill the two requirements in oral DNA vaccine delivery, efficient phagosomal escape and enhanced acid tolerance, thereby effectively modulating antitumor immune response (Scheme 1). To our knowledge, this is the first example of nanoparticle-modified bacterial delivery system for oral DNA vaccination in cancer immunotherapy in vivo. It may constitute a promising approach for engineering DNA vaccine delivery systems for a wide spectrum of immunotherapies in the future.

The morphology of the nanoparticle-coated *Salmonella* was first observed by scanning electron microscopy (SEM) to obtain direct insight into the interaction between *Salmonellae* and nanoparticles. As shown in Figure 1a, the uncoated naked *Salmonella* exhibited a typical rod shape with a smooth membrane surface, whereas polyplex nanoparticles were clearly observed to stick on the *Salmonella* surface in the case of nanoparticle-coated *Salmonellae*. Due to the electronegative nature of bacterial cell walls, the positively charged nanoparticles can be self-assembled onto *Salmonella* surface via electrostatic interaction, forming a dense coating layer over the rod-shaped *Salmonella*. The self-assembly approach of nanoparticle-coated bacteria in the current study is much simpler and more straightforward as compared to that of microbots where the surface premodification of both bacteria and nanoparticles is required before assembly.[28] The layer thickness is also found to increase with the nanoparticle coating concentration. LIVE/DEAD bacteria viability assay suggests the concentration of nanoparticle has a dose-dependent effect on the *Salmonella* viability because the strong electrostatic and hydrophobic interactions between polyplex nanoparticles and bacteria may

DOI: 10.1021/acs.nanolett.5b00570
Nano Lett. 2015, 15, 2732−2739

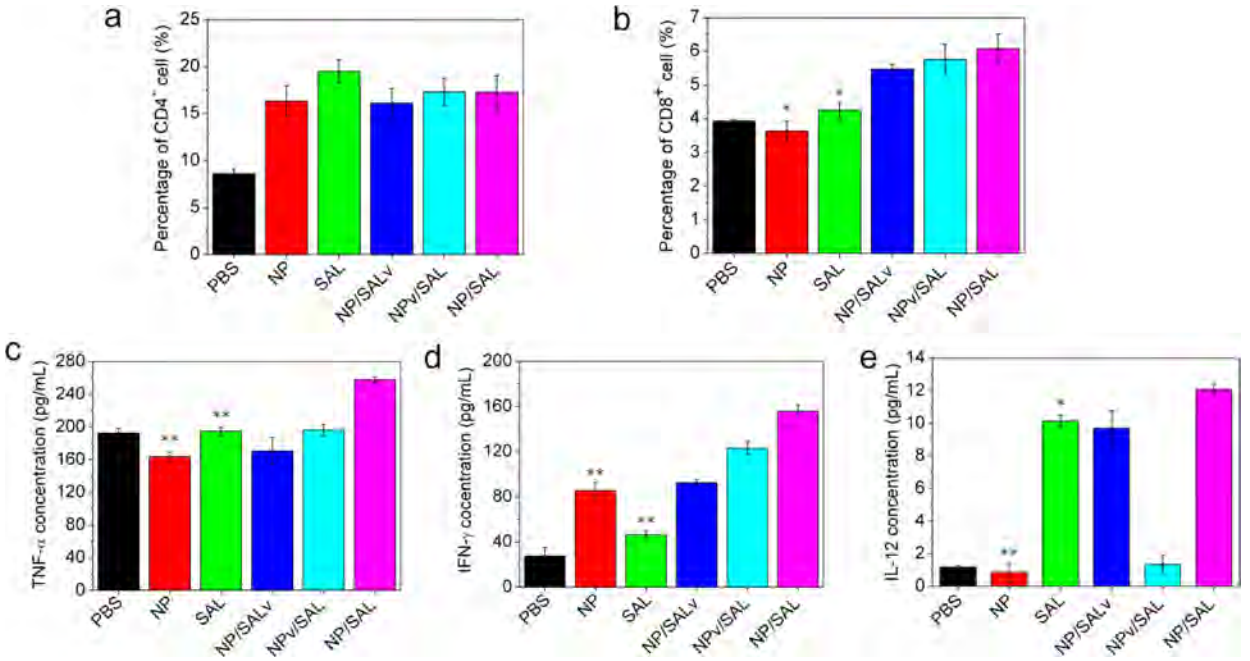

Figure 3. Induction of $CD4^+$ (a) and $CD8^+$ (b) T cells in C57BL/6J mice immunized with PBS, CP/pcDNA3.1-VEGFR2 (NP), *Salmonella*-pcDNA3.1-VEGFR2 (SAL), (CP/pcDNA3.1-VEGFR2)/*Salmonella*-pcDNA3.1 (NP/SALv), (CP/pcDNA3.1)/Salmonella-pcDNA3.1-VEGFR2 (NPv/SAL), and (CP/pcDNA3.1-VEGFR2)/*Salmonella*-pcDNA3.1-VEGFR2 (NP/SAL) on the B16 melanoma tumor model. The cells were isolated from the spleens and stained with PE-CD4 and FITC-CD8 antibodies. Quantification of cytokines TNF-α (c), IFN-γ (d), and IL-12 (e) harvested from the spleen cells after 3 weeks of successive immunization with different formations through the ELISA assay. NP/SALv represents hybrid of CP/pcDNA3.1-VEGFR2 complexes coating on *Salmonellae* loaded with pcDNA 3.1 (empty vector), whereas NPv/SAL stands for hybrid of CP/pcDNA3.1 complexes coating on *Salmonellae* loaded with pcDNA3.1-VEGFR2. NP/SAL stands for hybrid of CP/pcDNA3.1-VEGFR2 complexes coating on *Salmonellae* loaded with pcDNA 3.1-VEGFR2. The doses of pcDNA3.1-VEGFR2 in all formulations are equal. All data represent mean ± SD ($n = 3$, Student's t test, $^*P < 0.05$, $^{**}P < 0.01$, NP (or SAL) vs NP/SAL).

damage the cell wall of bacteria (Figure 1b).[37,38] Furthermore, although low concentration of nanoparticle coating was found to facilitate cellular uptake of *Salmonellae*, uptake efficiency dropped when higher coating concentration was applied (Supporting Information Figure S1). Therefore, NP/SAL with the minimum concentration of the polyplex coating was used in subsequent experiments.

During intracellular delivery process, poor phagosomal escape is often considered as the major barriers inhibiting antigen presentation of *Salmonella*.[39] We hypothesize that the nanoparticle coating may facilitate intracellular delivery and upregulate antigen expression. Cationic CP polymer was demonstrated to possess a strong acidic buffering capacity in our previous study due to the protonable amines in its backbone. As a result, we expect coating CP nanoparticles will also initiate a "proton-sponge" effect to rupture the phagosome. As shown in Figure 1c, after incubating the coated *Salmonella* with RAW264.7 at multiplicity of infection (MOI) ratio of 50:1 for 2 h, the nanoparticle-coated *Salmonella* was able to enter the cells and was trapped in the phagosome. This suggests that when *Salmonellae* are recognized and internalized by macrophages, the cationic nanoparticles carried by *Salmonellae* can be simultaneously internalized by macrophages. Confocal laser scanning microscopy (CLSM) study indicates that intracellular trafficking of the coated *Salmonella* (labeled by FITC over PC polymers) colocalize and sequester with phago/lysosome (labeled by red lysotracker) and only a small portion of green fluorescence is observed to spread out from LysoTracker, indicating NP/SAL hybrids are trapped by phagosomes (Supporting Information Figure S2). Furthermore, we examined the phagosomal pH induced by the naked and coated *Salmonella* through LysoSensor Yellow/Blue DND-160. The blue fluorescence indicates the neutral pH of the endosome, whereas green fluorescence represents acidic pH. As shown in Figure 2d, the coated *Salmonellae* can induce stronger green fluorescence than the naked *Salmonella*, suggesting a more acidic phagosome environment where the coated *Salmonella* is trapped. The protonation property of the CP polymer is likely to result in an acidic environment to facilitate phagosomal escape. Further studies show that the nanoparticle-coated *Salmonella* integrated with EGFP is able to initiate stronger GFP expression in different cell lines compared with uncoated ones (Supporting Information Figure S3), thereby confirming the ability of nanoparticle coating to enhance the antigen expression of *Salmonellae*. To improve the safety of bacteria as oral vaccines, attenuated *Salmonellae* generally exhibit reduced virulence, thereby displaying lower infection activity.[18] Supporting Information Figure S4 indicates that coating *Salmonellae* with either nonviral "gold standard" PEI (25 kDa)[28,32] or biodegradable poly-D,L-succinimide (PSI)-based PSI-NN′$_{0.85}$-NN$_1$ nanoparticles[40] can mediate efficient infection and induce strong GFP expression in RAW 264.7 cells. These results also demonstrate the effectiveness and versatility of this general approach to engineer efficient nanoparticle/bacteria hybrid delivery system. Therefore, nanoparticle coating plays an important role in facilitating endosomal escape and nanoparticle/*Salmonella* (NP/SAL) hybrids are expected to mediate efficient gene expression in vivo.

Although investigation of the transfection efficiency in vitro can identify promising materials for transfection, overcoming the harsh environment in the stomach and intestine before arriving at

DOI: 10.1021/acs.nanolett.5b00570
Nano Lett. 2015, 15, 2732−2739

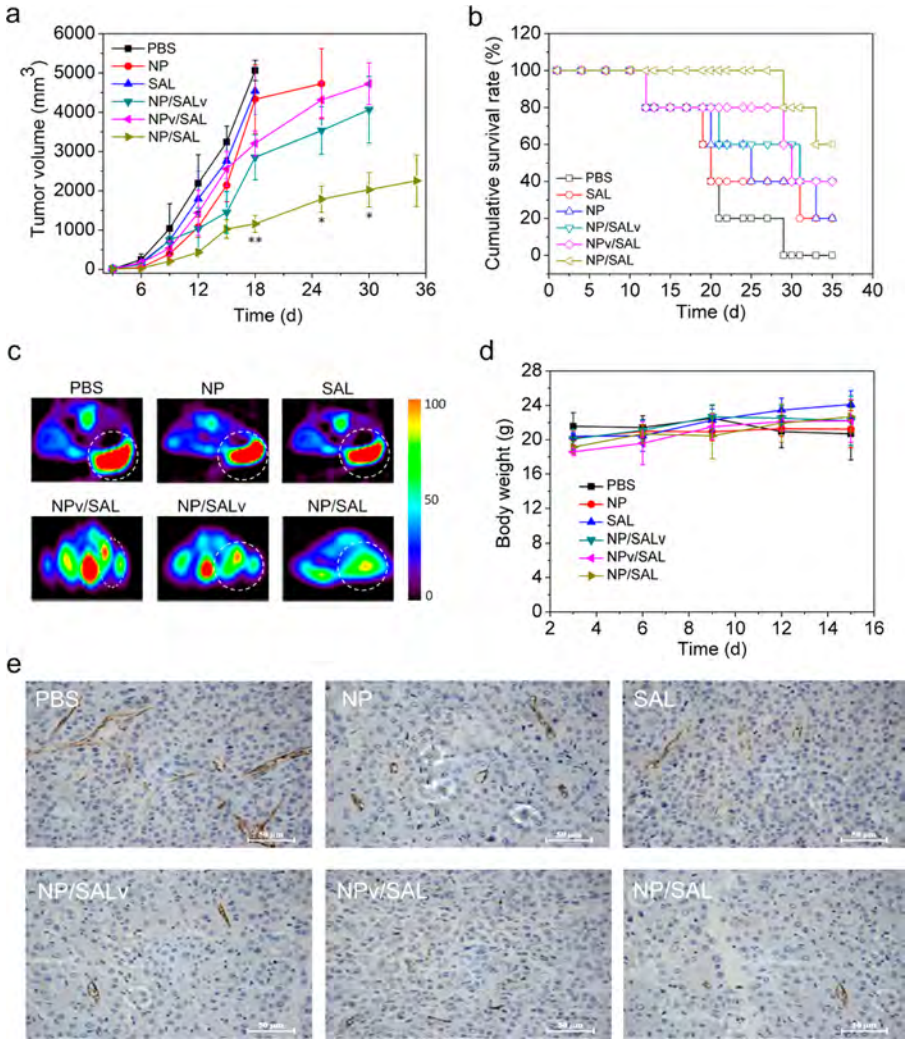

Figure 4. (a) Inhibition of tumor growth in C57BL/6-derived B16 melanoma tumor models orally vaccinated with PBS, NP, SAL, NP/SALv, NPv/SAL, and NP/SAL formulations. Data represent mean ± SD (n = 6, Student's t test, *P < 0.05, NP/SALv (or NPv/SAL) vs NP/SAL), **P < 0.01, NP (or SAL) vs NP/SAL). (b) Survival curves of tumor-bearing mice vaccinated with the different formulations. (c) PET images of in vivo tumor growth 18 days after the first treatment. The intensity is shown by the legend to the right. The circled area denotes the tumor position. (d) Average body weights of mice vaccinated with the different formulations in the B16 melanoma tumor model. Data represent mean ± SD (n = 6, Student's t test). (e) Immunohistochemical analysis of CD31 in the tumor slices of the B16 melanoma tumor model after immunization with different DNA vaccine formations. The scale bars represent 50 μm.

the targeted site of action remains a great challenge for effective oral DNA vaccine in vivo. An unavoidable reduction in the number of viable bacteria occurs during this process and only 10 to 25% of the ingested *Salmonella* can survive and reach the gut to initiate infection.[41] In order to be effective, it is essential to protect the *Salmonellae* from degradation when they pass through the stomach and upper intestine before reaching the gut in a sufficient amount. To mimic the stomach pH, we first analyze the effect of acidic pH on the viability of naked and coated *Salmonellae*. As shown in Figure 2a and c, there is almost no difference in terms of viability between the naked and coated *Salmonellae* at pH 7.4. In contrast, the relative viability of the naked *Salmonellae* dramatically drops to 10% at pH 3.0, whereas the relative viability of the coated *Salmonella* is about 58% at the same pH. We further measured the concentration of *Salmonellae* in blood after oral vaccination with the naked or coated *Salmonellae* (Figure 2b). Initially, slightly fewer coated *Salmonellae* were detected in the blood as compared with naked ones 30 min after oral administration. Afterward, the concentration of naked *Salmonellae* decreased significantly after another 30 min, becoming negligible after 2 h. In contrast, coated *Salmonellae* were found to have significantly higher blood concentration than uncoated *Salmonellae* in both time points (1 and 2 h). The above results demonstrate that whereas the tolerance of the *Salmonella* in the acidic environment can be significantly improved by surface coating with polyplex nanoparticles, the viability of uncoated *Salmonellae* remains extremely sensitive to gastric pH. We speculate that on one hand, strong buffering capacity of CP could partially protect bacteria from acid attack, thereby improving the tolerance of the *Salmonella* in the acidic condition. On the other hand, the coated NP layer may become more hydrophobic after nanoparticle coating, serving as a protective layer over the bacterial surface. In such a circumstance, the increased surface roughness of *Salmonellae* may reduce the direct contact between NP/SAL and acid fluids by forming a large contact angel between coated *Salmonella* surface and acid fluids. After oral administration, the higher blood concentration of viable bacteria with nanoparticle coating

DOI: 10.1021/acs.nanolett.5b00570
Nano Lett. 2015, 15, 2732−2739

strongly suggests that surface coating promotes the dissemination of the bacteria into blood, thus making the lymphoid tissue and systemic sites more accessible to the coated *Salmonella* to induce broad-based immune responses.[19] Meanwhile, the intestine toxicity results reveal that the small intestine treated with nanoparticle-coated *Salmonellae* exhibits well-defined heterochromatin and nucleoli in the epithelial cells and plasma cells, indicating the safety of the nanoparticle-coated *Salmonella* in small intestine in vivo (Figure 2d).

T cells play a critical role in the protective immunity against tumors. $CD4^+$ helper T cells play several important roles during the development and maintenance of $CD8^+$ cytotoxic T lymphocyte. Bacterium-based vaccines can induce systemic T-cell responses including polyfunctional cytokine-secreting $CD4^+$ and $CD8^+$ T-cells. Therefore, evoking the secretion of circulating tumor-specific T cells would promote antitumor immunity.[42] As shown in Figure 3a and b, the population of the $CD4^+$ T cells among the spleen administered with the PBS buffer is only 8.62%. The $CD4^+$ T cells significantly proliferate to the range of 16.11−19.30% when the mice were vaccinated with CP/pcDNA3.1-VEGFR2 (NP), *Salmonella*-pcDNA3.1-VEGFR2 (SAL), and (CP/pcDNA3.1-VEGFR2)/*Salmonella*-pcDNA3.1-VEGFR2 (NP/SAL). There is no distinct difference among NP, SAL, and NP/SAL, reflecting the naturally protective immunity. In the case of the $CD8^+$ T cells, the upregulated $CD8^+$ level was clearly evident when the tumor-bearing mice were immunized with all nanoparticle-coated *Salmonellae*, namely (CP/pcDNA3.1-VEGFR2)/*Salmonella*-pcDNA3.1 (NP/SALv), (CP/pcDNA3.1)/Salmonella-pcDNA3.1-VEGFR2 (NPv/SAL), and NP/SAL. Among these nanoparticle-coated *Salmonellae*, NP/SAL formulation is found to be most effective in activating $CD8^+$ T cells. These results strongly suggest that the nanoparticle coating can effectively stimulate the up-regulation of tumor-specific T cells thus boding well for the antitumor activity. Besides T-cell mediated antitumor immunity, different cytokines that are secreted in response to infection, inflammation, and immunity can exert inhibitory effects on tumor development and progression.[43] For example, interferon-γ (IFN-γ) is identified for its capacity to enhance tumor immunogenicity, promote mononuclear cell infiltration into the tumor tissue, and inhibit tumor angiogenesis.[44] Interleukin-12 (IL-12) is able to regulate the differentiation of naive T cells into TH1 cells,[45] and tumor necrosis factor-α (TNF-α) plays an important role for inducing hemorrhagic necrosis of solid tumors.[46] Thus, we quantify the cytokines level of IFN-γ, IL-12, and TNF-α in tumor-bearing mice after the administration of NP-coated *Salmonellae* by enzyme-linked immunosorbent assay (ELISA). As shown in Figure 3d, the NP/SAL possesses the strongest ability to produce TNF-α, which shows significantly higher level than NP or SAL, thereby suggesting that higher immune activation achieved by NP/SAL. The similar trends are also observed from IL-12 and TNF-α production (Figure 3c and e). Collectively, the results validate that the NP-coated *Salmonellae* are capable of improving antigen expression and antitumor immunity in an effective manner. Therefore, NP coating would exert positive effect on *Salmonellae* in activating antitumor immunity, which is expected to promote tumor suppression.

Angiogenesis is known as the formation of new blood vessels from pre-existing microvasculature, which is a complex and crucial process during tumor formation.[47,48] Many tumor masses secrete angiogenic factors such as vascular endothelial growth factor (VEGF) to promote blood vessel formation which eventually functions as a route for tumor metastasis. Among the VEGF receptor (VEGFR) family, VEGFR2 is essential for tumor angiogenesis and plays an important role in tumor growth, invasion, and metastasis.[49−51] Therefore, targeting the VEGFR2 pathway has become an attractive strategy for antiangiogenesis in cancer therapy.[52,53] In the current study, pcDNA3.1-VEGFR2 encoding autologous VEGFR2 was constructed and used as oral DNA vaccine for the study of tumor angiogenesis suppression (Supporting Information Figure S5). By preliminarily accessing antitumor activity on C57BL/6-derived B16 melanoma tumor models, we identified the formulation of NP/SAL (300 μg CP, 10^7 CFU bacteria) is most effective in inhibiting tumor growth and this formulation was then applied for the subsequent in vivo therapeutic experiments (Supporting Information Figure S6). As indicated in Figure 4a, tumor growth is greatly inhibited after oral immunization with NP/SAL hybrids loaded with pcDNA3.1-VEGFR2. The average tumor volume of the mice vaccinated with NP/SAL formulation is around 1000 mm^3 on the 18th day, which is at least 4 times and 3.7 times more potent than those vaccinated with naked *Salmonellae* (SAL) and polyplex nanoparticles (NP), respectively (Figure 4a, Supporting Information Figure S7). Interestingly, the intermediate inhibition effect was observed when the tumor-bearing mice were immunized with either NPv/SAL or NP/SALv formulation at the 18th day, and the average tumor volume of mice vaccinated with these formulations is more than two times larger as compared with those vaccinated with NP/SAL formulation at 30th day. Therapeutic outcomes can be maximized only when both nanoparticles and bacteria were loaded with DNA vaccine (NP/SAL), indicating a synergistic effect of two vectors. Furthermore, positron emission tomography (PET), which provides highly sensitive imaging modality for tumor diagnosis, is utilized to precisely measure the tumor volume. As shown in Figure 4c, the red color represents the highest intensity. The red color area decreases dramatically from uncoated *Salmonellae* to the coated ones. In the NP/SAL group, the weakest red fluorescence suggests the most effective vaccination against tumor growth. Generally, coated *Salmonellae* (NP/SAL, NPv/SAL and NP/SALv) are also more efficacious with respect to cumulative survival than PBS, SAL, NP formulations (Figure 4b). The survival study showed that 60% mice vaccinated with the formulation of NP/SAL survived entire 35-day study duration without tumor growth. Meanwhile, almost no body weight loss was observed over the mice vaccinated with the NP/SAL formulation, indicating its low systemic toxicity nature and minimum side effect (Figure 4d). These results strongly indicate the effectiveness of NP/SAL formulation as a safe oral DNA vaccine to inhibit tumor growth and to extend the survival time of tumor-bearing mice.

Cell apoptosis in the tumor tissues after treatment with various formulations were analyzed by H&E staining (Supporting Information Figure S8) and TUNEL assay (Supporting Information Figure S9). The H&E stained sections of tumor tissues from PBS and SAL groups appeared to be most hypercellular and exhibited nuclear polymorphism more obviously. Among these therapeutic groups, the tumor tissues from the vaccination with the NP/SAL formulation displayed the fewest tumor cells and the highest level of tumor necrosis. The TUNEL assay also showed that DNA vaccination with NP/SAL can induce much more TUNEL-positive cells. These results further validate the effectiveness of DNA vaccination through the oral delivery of pcDNA3.1-VEGFR2 by coated *Salmonellae*. Immunohistochemical analysis of CD31 reveals a distinct decrease in the vessel density of the tumor slice of the B16

DOI: 10.1021/acs.nanolett.5b00570
Nano Lett. 2015, 15, 2732−2739

melanoma tumor model after NP/SAL oral administration, when compared with the NP, SAL, and other formulations (Figure 4e). These results also provide important evidence for the effective tumor inhibition mediated by NP/SAL.

In conclusion, a new oral DNA vaccination approach mediated by cationic nanoparticle-coated bacteria for efficacious cancer immunotherapy is developed in this study. By coating attenuated *Salmonellae* with cationic CP nanoparticles, the protective nanoparticle coating layer is able to facilitate *Salmonellae* to effectively escape phagsomes, remarkably promotes the dissemination of the bacteria into blood, and significantly enhance the acid tolerance of *Salmonellae* in stomach and intestines. Oral delivery of DNA vaccine encoding autologous VEGFR2 by the hybrid vector shows remarkable T cell activation and cytokine production. Most importantly, successful inhibition of tumor growth is also achieved by this delivery strategy due to angiogenesis suppression in the tumor vasculature and tumor necrosis. This work demonstrates coating live attenuated bacteria with polymeric nanoparticles represents a promising strategy to engineer efficient and versatile DNA vaccine vectors. With a wide spectrum of bacterium choices, nanoparticles can be further tailored and functionalized for different delivery applications. This approach to delivering DNA vaccine may become a very promising therapeutic modality for treating a wide spectrum of cancers in the dawning era of personalized nanomedicine.

■ ASSOCIATED CONTENT

Supporting Information

Materials and methods, cellular uptake of coated or uncoated *Salmonellae* stained with SYTO9 in RAW 264.7 cells, intracellular distribution of coated *Salmonellae* after phagocytosis, GFP expression mediated by nanoparticle-coated *Salmonellae* and uncoated *Salmonellae*, GFP expression mediated by uncoated *Salmonellae* or *Salmonellae* coated with different nanoparticles, the plasmid structure of pcDNA3.1-VEGFR2, inhibition of tumor growth in C57BL/6-derived B16 melanoma tumor models orally vaccinated with PBS and nanoparticle-coated *Salmonellae* of different bacterium doses, dissected tumor tissues after successive 18 days of vaccination of different formulations in tumor-bearing mice, histological images of the tumor slices collected from the mice with H&E staining after oral DNA vaccinations, and references. This material is available free of charge via the Internet at http://pubs.acs.org.

■ AUTHOR INFORMATION

Corresponding Authors

*E-mail: pingyuan7@gmail.com.
*E-mail: tangguping@zju.edu.cn.

Author Contributions

⊥These authors contributed equally to this work.

Author Contributions

Q.H. and M.W. primarily performed the experiments. C.F., C.C., and W.F. assisted analysis of T cells and cytokines as well as evaluation of bacterial survival in vivo. M.Z. helped antitumor efficacy study in vivo. P.J.C. advised on the SEM study. Y.P. and G.T. designed the experiments, supervised the whole project, and wrote the paper. All authors have given approval to the final version of the manuscript.

Notes

The authors declare no competing financial interest.

■ ACKNOWLEDGMENTS

The authors greatly acknowledge Chinese National Natural Science Foundation (No. 21374098) for the financial support of this work. The authors also acknowledge Dr. Shahrouz Amini for drawing the Table of Content s for this manuscript.

■ REFERENCES

(1) Mellman, I.; Coukos, G.; Dranoff, G. *Nature* **2011**, *480*, 480−489.
(2) McDermott, D.; Lebbe, C.; Hodi, F. S.; Maio, M.; Weber, J. S.; Wolchok, J. D.; Thompson, J. A.; Balch, C. M. *Cancer Treat. Rev.* **2014**, *40*, 1056−1064.
(3) Palucka, K.; Banchereau, J. *Nat. Rev. Cancer* **2012**, *12*, 265−277.
(4) Xiang, R.; Luo, Y.; Niethammer, A. G.; Reisfeld, R. A. *Immunol. Rev.* **2008**, *222*, 117−128.
(5) Xiang, R.; Lode, H. N.; Chao, T. H.; Ruehlmann, J. M.; Dolman, C. S.; Rodriguez, F.; Whitton, J. L.; Overwijk, W. W.; Restifo, N. P.; Reisfeld, R. A. *Proc. Natl. Acad. Sci. U.S.A.* **2000**, *97*, 5492−5497.
(6) Bhavsar, M. D.; Amiji, M. M. *Expert Opin. Drug Delivery* **2007**, *4*, 197−213.
(7) Leong, K. W.; Sung, H. W. *Adv. Drug Delivery. Rev.* **2013**, *65*, 757−758.
(8) Ebensen, T.; Paukner, S.; Link, C.; Kudela, P.; de Domenico, C.; Lubitz, W.; Guzman, C. A. *J. Immunol.* **2004**, *172* (11), 6858−6865.
(9) Toussaint, B.; Chauchet, X.; Wang, Y.; Polack, B.; Le Gouellec, A. *Expert Rev. Vaccines* **2013**, *12*, 1139−1154.
(10) Yang, Y.; Hou, J.; Lin, Z.; Zhuo, H.; Chen, D.; Zhang, X.; Chen, Y.; Sun, B. *Cell Mol. Immunol.* **2014**, *11*, 184−196.
(11) Gardlik, R.; Fruehauf, J. H. *IDrugs* **2010**, *13*, 701−706.
(12) Reisfeld, R. A.; Niethammer, A. G.; Luo, Y.; Xiang, R. *Immunol. Rev.* **2004**, *199*, 181−90.
(13) Niethammer, A. G.; Xiang, R.; Becker, J. C.; Wodrich, H.; Pertl, U.; Karsten, G.; Eliceiri, B. P.; Reisfeld, R. A. *Nat. Med.* **2002**, *8*, 1369−1375.
(14) Loessner, H.; Endmann, A.; Leschner, S.; Bauer, H.; Zelmer, A.; zur Lage, S.; Westphal, K.; Weiss, S. *Int. J. Med. Microbiol.* **2008**, *298*, 21−26.
(15) Toso, J. F.; Gill, V. J.; Hwu, P.; Marincola, F. M.; Restifo, N. P.; Schwartzentruber, D. J.; Sherry, R. M.; Topalian, S. L.; Yang, J. C.; Stock, F.; Freezer, L. J.; Morton, K. E.; Seipp, C.; Haworth, L.; Mavroukakis, S.; White, D.; MacDonald, S.; Mao, J.; Sznol, M.; Rosenberg, S. A. *J. Clin. Oncol.* **2002**, *20*, 142−152.
(16) Thamm, D. H.; Kurzman, I. D.; King, I.; Li, Z.; Sznol, M.; Dubielzig, R. R.; Vail, D. M.; MacEwen, E. G. *Clin. Cancer Res.* **2005**, *11*, 4827−4834.
(17) Jia, L. J.; Wei, D. P.; Sun, Q. M.; Huang, Y.; Wu, Q.; Hua, Z. C. *Cancer Sci.* **2007**, *98*, 1107−1112.
(18) Jones, B. D.; Falkow, S. *Annu. Rev. Immunol.* **1996**, *14*, 533−561.
(19) Bao, S.; Beagley, K. W.; France, M. P.; Shen, J.; Husband, A. J. *Immunol.* **2000**, *99*, 464−472.
(20) Gorden, J.; Small, P. L. *Infect. Immun.* **1993**, *61*, 364−367.
(21) Kaufmann, S. H.; Hess, J. *Immunol. Lett.* **1999**, *65*, 81−84.
(22) Chorobik, P.; Czaplicki, D.; Ossysek, K.; Bereta, J. *Acta Biochim. Polym.* **2013**, *60*, 285−97.
(23) Magennis, E. P.; Fernandez-Trillo, F.; Sui, C.; Spain, S. G.; Bradshaw, D. J.; Churchley, D.; Mantovani, G.; Winzer, K.; Alexander, C. *Nat. Mater.* **2014**, *13*, 748−755.
(24) Feng, X.; Yang, G.; Liu, L.; Lv, F.; Yang, Q.; Wang, S.; Zhu, D. *Adv. Mater.* **2012**, *24*, 637−641.
(25) Chen, A. Y.; Deng, Z.; Billings, A. N.; Seker, U. O. S.; Lu, M. Y.; Citorik, R. J.; Zakeri, B.; Lu, T. K. *Nat. Mater.* **2014**, *13*, 515−523.
(26) Lee, C. H.; Lin, Y. H.; Hsieh, J. L.; Chen, M. C.; Kuo, W. L. *Int. J. Cancer* **2013**, *132*, 717−725.
(27) Zhu, C.; Yang, Q.; Lv, F.; Liu, L.; Wang, S. *Adv. Mater.* **2013**, *25*, 1203−1208.
(28) Akin, D.; Sturgis, J.; Ragheb, K.; Sherman, D.; Burkholder, K.; Robinson, J. P.; Bhunia, A. K.; Mohammed, S.; Bashir, R. *Nat. Nano.* **2007**, *2*, 441−449.
(29) Mintzer, M. A.; Simanek, E. E. *Chem. Rev.* **2009**, *109*, 259−302.

DOI: 10.1021/acs.nanolett.5b00570
Nano Lett. 2015, 15, 2732−2739

(30) Yin, H.; Kanasty, R. L.; Eltoukhy, A. A.; Vegas, A. J.; Dorkin, J. R.; Anderson, D. G. *Nat. Rev. Genet.* **2014**, *15*, 541−555.
(31) Pietersz, G. A.; Tang, C. K.; Apostolopoulos, V. *Mini Rev. Med. Chem.* **2006**, *6*, 1285−1298.
(32) Boussif, O.; Lezoualc'h, F.; Zanta, M. A.; Mergny, M. D.; Scherman, D.; Demeneix, B.; Behr, J. P. *Proc. Natl. Acad. Sci. U.S.A.* **1995**, *92*, 7297−7301.
(33) Tang, G. P.; Guo, H. Y.; Alexis, F.; Wang, X.; Zeng, S.; Lim, T. M.; Ding, J.; Yang, Y. Y.; Wang, S. *J. Gene Med.* **2006**, *8*, 736−744.
(34) Hu, Q. D.; Tang, G. P.; Chu, P. K. *Acc. Chem. Res.* **2014**, *47*, 2017−2025.
(35) Ping, Y.; Hu, Q.; Tang, G.; Li, J. *Biomaterials* **2013**, *34*, 6482−6494.
(36) Hu, Q. D.; Fan, H.; Ping, Y.; Liang, W. Q.; Tang, G. P.; Li, J. *Chem. Commun.* **2011**, *47*, 5572−5574.
(37) Yang, C.; Ding, X.; Ono, R. J.; Lee, H.; Hsu, L. Y.; Tong, Y. W.; Hedrick, J.; Yang, Y. Y. *Adv. Mater.* **2014**, *26*, 7346−7351.
(38) Liu, M.; Li, Z. H.; Xu, F. J.; Lai, L. H.; Wang, Q. Q.; Tang, G. P.; Yang, W. T. *Biomaterials* **2012**, *33*, 2240−2250.
(39) Parsa, S.; Pfeifer, B. *Mol. Pharmaceutics* **2007**, *4*, 4−17.
(40) Shen, J.; Zhao, D. J.; Li, W.; Hu, Q. L.; Wang, Q. W.; Xu, F. J.; Tang, G. P. *Biomaterials* **2013**, *34*, 4520−4531.
(41) Del Piano, M.; Morelli, L.; Strozzi, G. P.; Allesina, S.; Barba, M.; Deidda, F.; Lorenzini, P.; Ballare, M.; Montino, F.; Orsello, M.; Sartori, M.; Garello, E.; Carmagnola, S.; Pagliarulo, M.; Capurso, L. *Dig. Liver Dis.* **2006**, *38* (Suppl 2), S248−255.
(42) Bolhassani, A.; Zahedifard, F. *Int. J. Cancer* **2012**, *131*, 1733−1743.
(43) Li, D.; Li, Y.; Xing, H.; Guo, J.; Ping, Y.; Tang, G. *Adv. Funct. Mater.* **2014**, *24*, 5482−5492.
(44) Beatty, G. L.; Paterson, Y. *Immunol. Res.* **2001**, *24*, 201−210.
(45) Trinchieri, G.; Pflanz, S.; Kastelein, R. A. *Immunity* **2003**, *19*, 641−644.
(46) Carswell, E. A.; Old, L. J.; Kassel, R. L.; Green, S.; Fiore, N.; Williamson, B. *Proc. Natl. Acad. Sci. U.S.A.* **1975**, *72*, 3666−3670.
(47) Folkman, J. *Nat. Med.* **1996**, *2*, 167−168.
(48) Eberhard, A.; Kahlert, S.; Goede, V.; Hemmerlein, B.; Plate, K. H.; Augustin, H. G. *Cancer Res.* **2000**, *60*, 1388−1393.
(49) Cross, M. J.; Claesson-Welsh, L. *Trends Pharmacol. Sci.* **2001**, *22*, 201−207.
(50) Ferrara, N. *Curr. Opin. Biotechnol.* **2000**, *11*, 617−624.
(51) Taraboletti, G.; Margosio, B. *Curr. Opin. Pharmacol.* **2001**, *1*, 378−384.
(52) Grothey, A.; Galanis, E. *Nat. Rev. Clin. Oncol.* **2009**, *6*, 507−518.
(53) Potente, M.; Gerhardt, H.; Carmeliet, P. *Cell* **2011**, *146*, 873−887.

DOI: 10.1021/acs.nanolett.5b00570
Nano Lett. 2015, 15, 2732−2739

Supporting Information

Engineering Nanoparticle-Coated Bacteria as Oral DNA Vaccines for Cancer Immunotherapy

Qinglian Hu,[†1] Min Wu,[†1] Chun Fang,[‡] Changyong Cheng,[‡] Mengmeng Zhao,[†] Weihuan Fang,[‡] Paul K. Chu,[‖] Yuan Ping,[§,] and Guping Tang[†,*]*

[†]Institute of Chemical Biology and Pharmaceutical Chemistry, Zhejiang University, Hangzhou 310028, China

[‡]College of Animal Science, Zhejiang University, Hangzhou 310028, P. R. China

[‖]Department of Physics and Materials Science, City University of Hong Kong, Tat Chee Avenue, Kowloon, Hong Kong, China

[§]School of Materials Science and Engineering, Nanyang Technological University, Singapore 639798, Singapore

[1] These authors contributed equally to this work

[*]Corresponding Author: pingyuan7@gmail.com (Y. P.); tangguping@zju.edu.cn (G. T.)

1. Materials and methods

Materials. Dulbecco's Modified Essential Medium (DMEM) is a commercial product provided by National University Medical Institutes (Singapore) and Milli-Q water was supplied by Milli-Q Plus System (Millipore Corporation, Breford, United States). The fetal bovine serum (FBS) and trypsin-EDTA solution were purchased from Gibco (Life Technologies, AG, Switzerland) and fluorecein isothiocyanate isomer I (FITC) was purchased from Sigma-Aldrich (St. Louis, MO, USA). LysoTracker Red and Hochest 33342 were obtained from Beyotime Institute of Biotechnology (Haimen, Jiangsu, China). L13152 LIVE/DEAD BacLight Bacterial Viability Kit, Alexa Fluor 568 phalloidin, and LysoSensor Yellow/Blue DND-160 were obtained from Invitrogen (USA). Phycoerythrin (PE) labeled rat anti-mouse $CD4^+$ and FITC labeled rat anti-mouse $CD8^+$ antibody were purchased from Keygen Biotech (Naijing China). Mouse interferon-γ (IFN-γ), interleukin 12 (IL12) and tumor necrosis factor α (TNF-α) ELISA Kits were supplied by from Boster (Pleasanton, USA). The DeadEndTM colorimetric TUNEL system was obtained from Promega and blood vessel staining kit was obtained from Merck Millipore.

Cell culture. Mouse melanoma cells B16F10, human intestinal Caco-2, and mouse macrophage-like RAW264.7 cells were provided by American Type Culture Collection (ATCC). The cells were cultured in DMEM (Invitrogen, Carlsbad, CA) containing 10% heat-inactivated FBS (Invitrogen), 100 U mL^{-1} penicillin, and 100 μg mL^{-1} streptomycin (Thermo Scientific) and maintained in a humidified incubator at 37 °C with 5% CO_2. Before the experiments, the cells were pre-cultured until confluence was reached. The peritoneal macrophage was purified according to the conventional protocol from healthy male ICR mice that were purchased from the animal center of Zhejiang Academy of Medical Science.

Plasmid DNA and bacteria strain. The murine vascular endothelial growth factor receptor 2 (VEGFR2) was cloned into pcDNA3.1 vector to construct the pcDNA3.1-VEGFR2 plasmid, which was provided by Changsha Yingrun Biotechnology. The pcDNA3.1 empty vector and pEGFP (encoding enhanced green fluorescence protein, EGFP) plasmid was a gift from the Institute of Immunology, Second Military Medical University, Shanghai, P. R. China. The attenuated *Salmonella* strain, EGFP, pcDNA3.1-VEGFR2, and pcDNA3.1 vector recombinant *Salmonellae* were provided by College of Animal Sciences, Zhejiang University, P. R. China.

Preparation of nanoparticle-coated bacteria and SEM characterization. The EGFP, pcDNA3.1-VEGFR2, and pcDNA3.1 vector transformed attenuated *Salmonellae* were routinely grown at 37 °C in LB medium and supplemented with 100 μg/mL of ampicillin overnight. Afterwards, the bacteria were collected and the optical density (OD) of the bacterial suspension was adjusted to 0.85, which corresponded to the bacteria concentration of 3×10^9 CFU/mL. The details about the synthesis and characterization of CP were described in our previous publication.[1] The CP solution was added to the plasmid DNA solutions with the same volume, mixed, and incubated for 20 min at room temperature to form the cationic polyplexes with the N/P ratio of 25. The bacteria solution was diluted to 1×10^8 CFU/mL and 20 μL of the bacterium solution were added to the polyplex solution and incubated for 20 min to form the cationic polyplex coated *Salmonellae*.

The morphology of the uncoated and coated *Salmonella* was examined by SEM (Hitachi S-4300, Japan). Both *Salmonella* pellets were collected, fixed with 1% glutaraldehyde at 4°C for 2 hour, and centrifuged at 5000 g for 5 min. After removal of the supernatant, the bacteria pellets were suspended in sterile water. The pellets were washed 3 times, and 5 μL of the bacteria suspensions were added to the clean silicon slices. After the specimens were dried, ethanol with concentrations of 70%, 90%, and 100% was used sequentially to dehydrate the pellet for 10 min. After the ethanol residue was completely removed, the specimens were coated with platinum before observation under SEM.

Bacteria viability assay. The effect of the polyplex concentration on the viability of attenuated *Salmonella* was evaluated by a LIVE/DEAD BacLight bacterial viability kit according to the manufacturer's protocol. The assay kit included a green fluorescence dye $SYTO_9$ marking viable bacterial cells and red dye PI for detection of dead bacterial cells. Polyplex solutions with different concentrations were added to the bacteria solution and mixed thoroughly with the dye solution for 15 min in darkness at room temperature. 5 μL of the stained bacterium suspension was placed between a slide and an 18 mm^2 coverslip for examination by fluorescence microscopy.

Intracellular trafficking of polyplex-coated *Salmonella*. The cellular uptake of the naked and coated *Salmonellae* in RAW264.7 cell lines was evaluated. The uncoated and coated *Salmonellae* were first stained with $SYTO_9$ in darkness for 15 min before the assay. The cells were seeded at a density of 4×10^4/well on 24-well plates and grown for 18 h at 37°C in a humidified 5% CO_2 incubator. The medium was replaced with 0.3 mL of fresh serum-free

medium and 100 μL of the stained bacteria at MOI ratio of 50 were added to each well. After 2 hours, the medium was replaced by the serum free media containing the 2×penicillin-streptomycin solution for 2 hours to eliminate extracellular bacteria. The cells were then washed twice with PBS and stained with Alexa Fluor® 568 phalloidin and Hoechst 33245, respectively.

The ability of the nanoparticle-coated *Salmonellae* to escape from lysosome was evaluated as follows. The FITC-conjugated CP was used to parepare fluoresncent nanoparticle, which was used then to coat *Salmonellae.*FITC-labled nanoparticle was obtained by adding 50 mg of CP to 2.5 μmol of the FITC isomer in 5 mL of a 1:1 DMSO/water mixture, and the solution was stirred in darkness for 2 h and the unreacted FITC residues were removed by dialysis using dialysis membrane (molecular weight cut off 8000) in distilled water for 2 days. The purified FITC-conjugated CP was then used to prepare polymer/DNA complexes at N/P ratio of 25. The RAW 267.4 and peritoneal macrophage were seeded at a density of 4×10^4/well on 24-well plates for 24 hours. The protocols of FITC-PC/pDNA coated bacterial infection were the same as described previously. The cells were rinsed and incubated in the medium containing 100 nM LysoTracker for 1 h. The cells were fixed with fresh 4% paraformaldehyde and then treated with 10 μg/mL Hoechst 33245 in PBS for 10 min. The images were taken on a confocal scanning laser microscope (CLSM, Radiance 2100, Bio-Rad).

The phago/lysosomal pH change in the peritoneal macrophage after infection by naked and coated bacteria was monitored by LysoSensor Yellow/Blue DND-160. The peritoneal macrophage was purified according to the conventional protocol from Healthy male ICR mice which were purchased from the animal center of Zhejiang Academy of Medical Science. The peritoneal macrophage was seeded at a density of 4×10^4/well on 24-well plates for 24 hours. After bacterial infection, the cells were rinsed and incubated in the medium containing 1 μm LysoSensor Yellow/Blue DND-160 for 1 h. The cells were fixed with fresh 4% paraformaldehyde and washed twice. The images were taken on a confocal scanning laser scanning microscope (CLSM, Radiance 2100, Bio-Rad).

For TEM observation of the cell sections, the RAW 264.7 cells were seeded on a 6-well plate at a certain density (1×10^6) cells per well and cultured for 18 hour. The medium was replaced with 0.3 mL of the fresh serum-free medium and 100 mL of freshly prepared polyplex-coated *Salmonellae* at multiplicity of infection (MOI) ratio of 50 (bacteria/cell) were added to each well. After transfection for 2 h, the medium was replaced by the serum free medium containing the 2×penicillin-streptomycin solution for 2 hours to eliminate

extracellular bacteria. The cells were washed twice with PBS, trypsizined, centrifuged, and fixed with 2.5% glutaraldehyde at 4 °C overnight. The samples were washed with PBS and post-fixed with 1% osmium tetroxide for 2 h prior to dehydration in a graded series of ethanol. All the specimens were embedded, sliced to a thickness between 50 and 70 nm, and collected on 200-mesh copper grids. The samples were stained with uranyl acetate and lead citrate prior to TEM observation.

Bacteria protection experiment. A single colony of EGFP-transfected *Salmonella* on a solid Luria-Bertani (LB) agar plate was transferred to 5 mL of the liquid LB culture medium in the presence of 50 μg/mL Kanamycin B and grown at 37 °C for 12 h. The bacteria were harvested by centrifuging (5,000 g for 5 min) and washing by PBS three times. The bacteria solution were added to the polyplex solution and incubated for 20 min to form the cationic nanoparticle-coated *Salmonellae* before the bacteria suspension was diluted (4,000 folds) with PBS buffer solution. The solution was centrifuged again, and the supernatant was discarded and remaining *Salmonellae* were re-suspended in the PBS buffer solution. The optical density (OD_{600}) of the bacteria suspension was adjusted to 0.85. The solution was divided into two parts equally. One portion was centrifuged and re-suspended in the pH 3.0 sodium acetate - acetic acid buffer solutions (0.1M), and the pH was measured after resuspension. The other portion of bacteria solution was kept in PBS buffer solution (pH 7.4). The bacteria solution was then diluted to 1×10^8 CFU/mL by pH 3.0 or 7.4 buffer solution. A 100 μL portion of the diluted bacteria was spread on the solid LB agar plate and the colonies formed after incubation for 12-16 h at 37 °C were counted.

With regard to the blood bacterium concentration assay, healthy male ICR mice (4-6 weeks old) were purchased from the animal center of Zhejiang Academy of Medical Sciences. The animal experiments were performed according to the Guidelines for Animal Care and Use Committee, Zhejiang University. The bacterium dose for the oral vaccine was 1×10^8 CFU per mouse. At different time point after oral vaccination, the blood samples were harvested from the eyes of the mice and then the mice were euthanized. To avoid blood coagulation, the tubes were treated with heparin before harvesting. The blood samples were diluted 4 folds in PBS. A 100 μL portion of the diluted blood solution was spread on the solid LB agar plate and the colonies formed after incubation for 12-16 h at 37 °C were counted.

Oral vaccination and antitumor activity. The B16F10 cells were injected subcutaneously (100 μL injection volume; 5 million cells) to the left abdominal of C57BL/6 mice. When the

tumor grew to a volume of 10-12 mm^3 in 7 days, the mice were randomly assigned to 6 groups (6 mice for each group): Normal PBS, CP/pcDNA3.1-VEGFR2 (CP), *Salmonella*-pcDNA3.1-VEGFR2 (SAL), (CP/pcDNA3.1-VEGFR2)/*Salmonella*-pcDNA3.1 (NP/SALv), (CP/pcDNA3.1)/Salmonella-pcDNA3.1-VEGFR2 (NPv/SAL), (CP/pcDNA3.1-VEGFR2)/*Salmonella*-pcDNA3.1-VEGFR2 (NP/SAL). Each group contains an equivalent dose of 30 μg recombinant plasmid, CP (300 μg) or/and *Salmonellae* (10^7 CFU) in a total volume of 100 μL. The treatment was performed every three day for consecutive 18 days. To avoid the extreme low pH of stomach (pH 1-2), the mice were subjected to starvation for a few hours before oral administration. The tumor growth was monitored by measuring the tumor length and width with a calliper and the tumor volume was calculated as follows: tumor volume V (mm^3) =π/6× length (mm) × width $(mm)^2$. Three mice from each group were sacrificed 18 days after first injection. The tumors from sacrificed mice were dissected, weighed, and imaged.

Positron Emission Tomography (PET) Imaging. ^{18}F-fluorodeoxyglucose (^{18}F-FDG) micro PET imaging was performed on a micro PET R4 scanner (Concorde Microsystems, Knoxville, TN, USA) which consisted of a 15 cm diameter ring of 96 position-sensitive γ-ray scintillation detectors, providing a 10 cm transaxial and a 7 cm axial field of view with an image resolution of <1.8 mm. The trans-axial image planes were separated by 1.2 mm. In brief, 1.5 min halothane gas anesthesia was performed and the mice were intravenously injected with 500 mCi/mmol ^{18}F-FDG *via* abdominal injection. The mice were put in cages and placed in a room with minimal ambient noise. They were allowed to move around for 50 min after tracer injection. Subsequently, the animals were placed in the micro PET scanner under halothane gas anesthesia (5% induction and 1.5% for maintenance). Static data acquisition was performed for 10 min in the 3D mode.

$CD8^+$ and $CD4^+$ T cell analysis and cytokine quantification. The C57BL/6 mice harboring B16F10 tumor model were orally administered with PBS, NP, SAL, NPv/SAL, NP/SALv and NP/SAL 3 times within 2 weeks. Three mice per group were euthanized and the spleens were harvested and crushed by 200 mesh nylon net. The collected splenocytes were suspended in 5 ml of the EZ-Sep mouse 1× lymphocyte separation medium (Eton bioscience Inc, USA) and centrifuged for 30 min at 800 g. The cells in the intermediate layer were collected, washed three times with PBS, and then centrifuged for 10 min at 250 g. The spleen cells were divided into two groups, one for the T cell analysis and the other for cytokine quantification. In the T

cell test, the spleen cells were re-suspended in the PBS buffer at 1×10^7/mL and 1% BSA solution was added to block nonspecific labeling due to FcR binding. The PE rat anti-mouse $CD4^+$ and FITC labeled rat anti-mouse $CD8^+$ antibody (0.25 mg/10^6 cells) were cultured with the spleen cells in darkness for 30 min. The cells were washed and a minimum of 10,000 cells were analyzed in each sample using an EPICS XL flow cytometer (Beckman-Coulter, USA).

For cytokine quantification, the harvested spleen cells were suspended in 5 mL of the RPMI 1640 culture medium supplemented with 10 % FBS for 24 h. The supernatants were collected and cytokines were quantified using Mouse TNF-α, IL-12, and IFN-γ ELISA Kits (Life technologies, USA).

Tissue immunohistological evaluation. In the histological assay, the small intestine and tumor tissues were fixed in 4% paraformaldehyde for 24 h. The specimens were dehydrated in graded ethanol, embedded in paraffin, and cut into 5 mm thick sections. The fixed sections were deparaffinized and hydrated according to a standard protocol and stained with hematoxylin and eosin (HE) for microscopic observation.

Apoptosis of the tumor cells in the mice after treatments was determined by the TUNEL method according to the manufacturer's instructions. The vascular labelling was stained with anti-CD31 antibody and hematoxylin and all the sections were examined on a Leica (DMLB&DMIL) microscope.

Statistical Analysis. All the experiments were repeated at least three times. The data were presented as means ± standard deviations. Statistical significance was evaluated by the Student's t-test when two groups were compared.

Reference:

1. Ping, Y.; Hu, Q.; Tang, G.; Li, J. *Biomaterials* **2013,** *34,* 6482-6494.

2. Figures

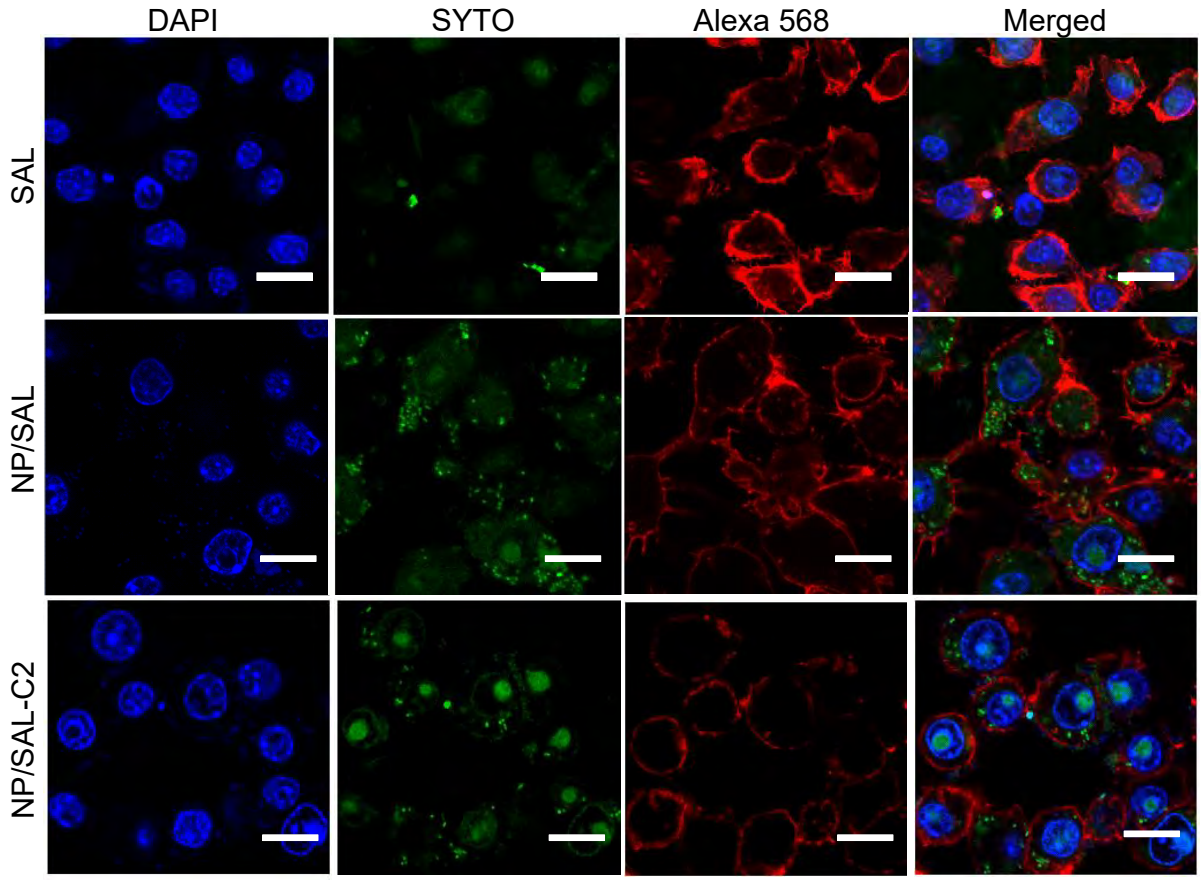

Figure S1. Cellular uptake of coated or uncoated *Salmonellae* stained with SYTO9 in RAW 264.7 cells. Cell nuclei were stained with blue-fluorescent Hoechst 33245 and the cell cytoskeleton F-actins were labeled with red-fluorescent Alexa Fluor® 568 phalloidin. The scale bars represent 20 µm.

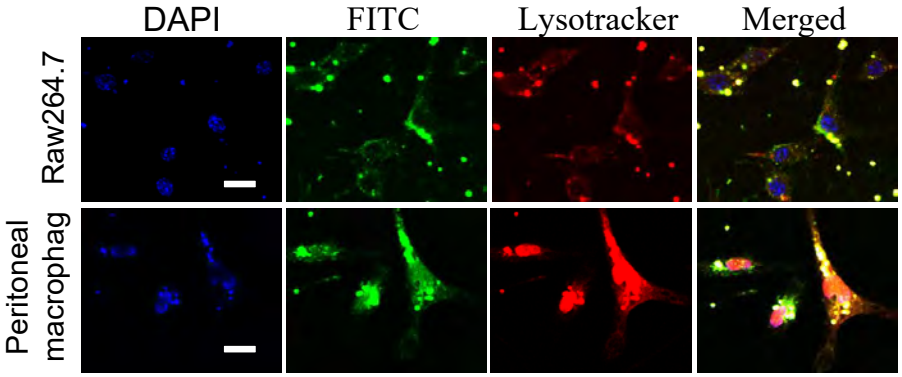

Figure S2. Intracellular distribution of coated *Salmonellae* after phagocytosis. The PC polymers are labeled with green FITC and phgo/lysosomal are labeled with red LysoTracker. The cell nuclei were stained with DAPI. The scale bars represent 20 µm.

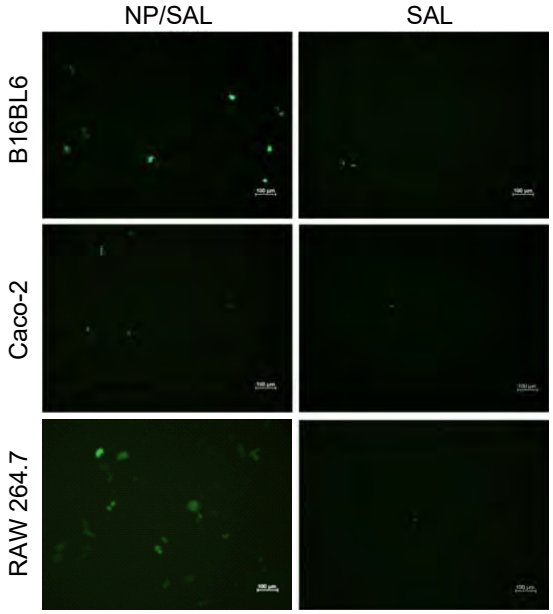

Figure S3. GFP expression mediated by nanoparticle-coated *Salminellae* (NP/SAL, left pane) and uncoated *Salmonella* (SAL, right pane) in B16BL6, CACO-2, and RAW 264.7 cell lines. The scale bars represent 100 µm.

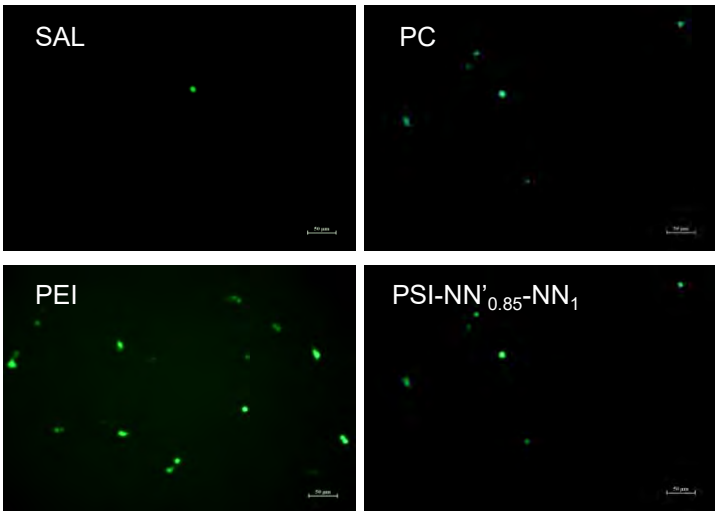

Figure S4. GFP expression mediated by uncoated *Salmonellae* or *Salmonellae* coated with different nanoparticles self-assembled from cationic polymers and plasmid DNA in RAW 264.7 cell lines. The scale bars represent 100 µm.

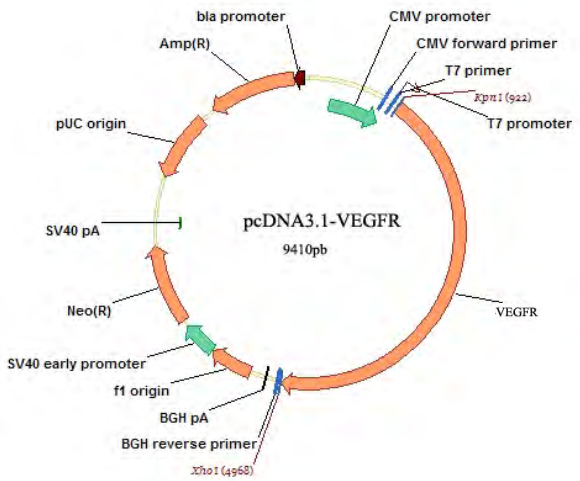

Figure S5. The plasmid structure of pcDNA3.1-VEGFR2.

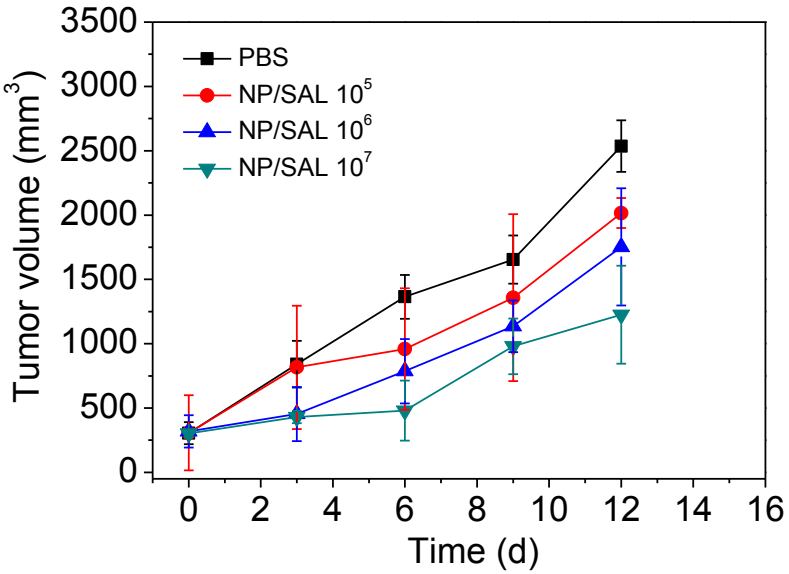

Figure S6. Inhibition of tumor growth in C57BL/6-derived B16 melanoma tumor models orally vaccinated with PBS and nanoparticle-coated *Salmonellae* of different bacterium doses. Whereas the dose of the CP is fixed at 300 μg, different doses of *Salmonellae* (10^5, 10^6, and 10^7 CFU) are mixed with the CP nanoparticles to form the hybrid NP/SAL formulation. Data represent mean ± SD (n = 6).

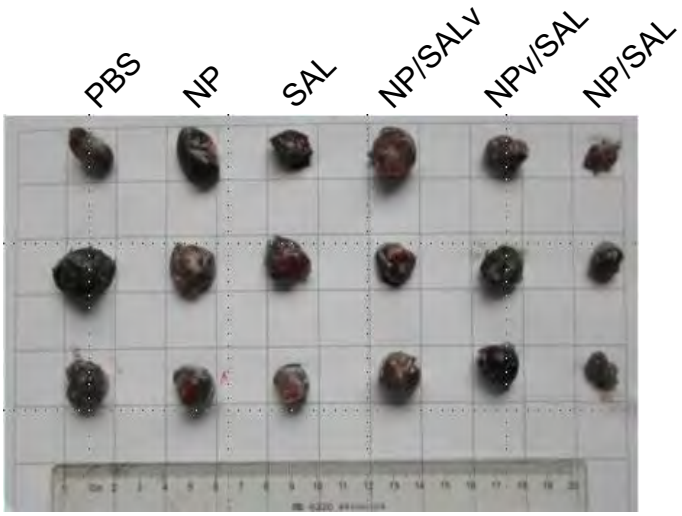

Figure S7. Dissected tumor tissues after successive 18 days of vaccination of different formulations in tumor-bearing mice. The size of each grid is approximately 2 cm × 2 cm.

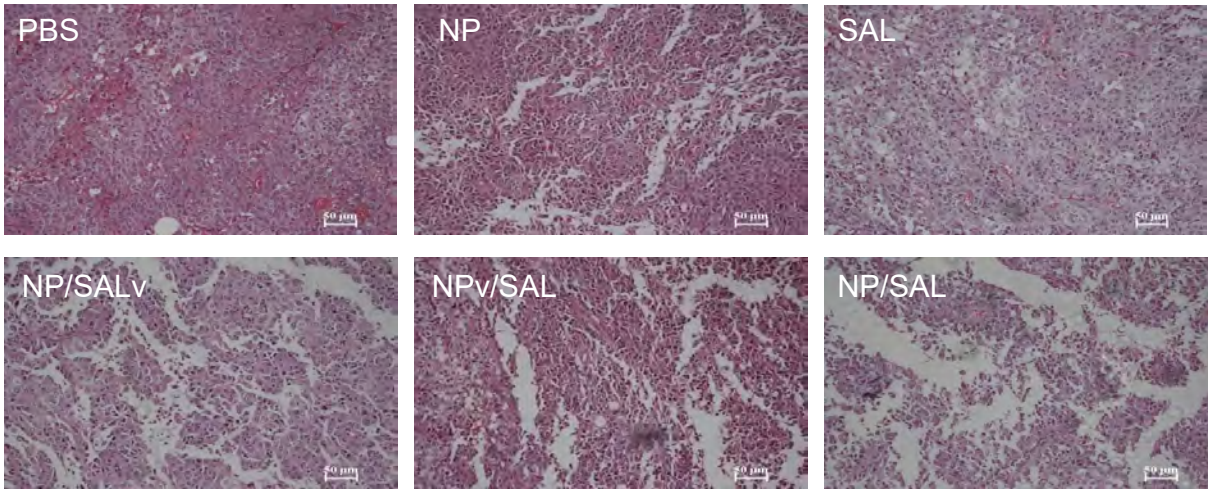

Figure S8. Histological images of the tumor slices collected from the mice with H&E staining after oral DNA vaccinations. All scale bars represent 50 μm.

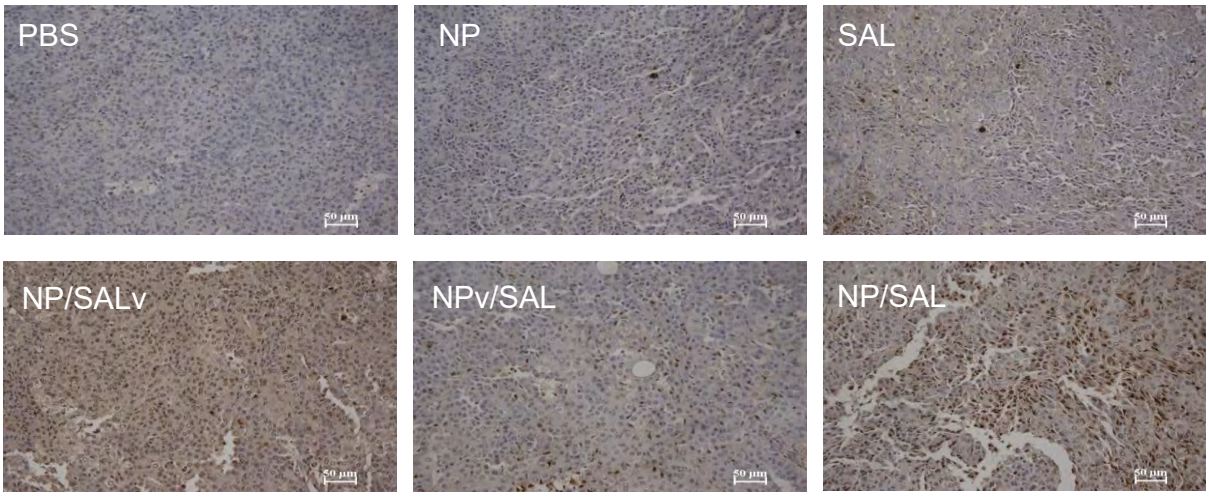

Figure S9. Terminal deoxynucleotidyl transferase dUTP nick end labeling (TUNEL) assay of tumor slices collected from the mice after oral DNA vaccinations. All scale bars represent 50 μm.